Theor Chem Acc (2016) 135:69
DOI 10.1007/s00214-016-1837-5

REGULAR ARTICLE

# Singlet–triplet excitation energies of substituted phenyl cations: a G4(MP2) and G4 theoretical study

**Sierra Rayne**[1] · **Kaya Forest**[2]

Received: 12 December 2015 / Accepted: 3 February 2016 / Published online: 27 February 2016


**Abstract** Singlet–triplet adiabatic excitation energies ($AE_{S-T}$) of the parent and variously substituted phenyl cations, as well as the parent benzannelated derivatives up to anthracenyl, were calculated at the G4(MP2) and G4 levels of theory. The G4(MP2)/G4 $AE_{S-T}$ estimates range up to 40 kJ/mol higher than prior density functional theory (DFT)-based predictions for these cations and suggest that $AE_{S-T}$ and ground state multiplicity structure–property trends for phenyl cations previously proposed in the literature need to be re-assessed at higher levels of theory. In general, Hartree–Fock, DFT, and semiempirical methods do a poor job describing the singlet–triplet excitation energetics of these systems. Only modest effects of different solvation models (SMD, IEF-PCM, and C-PCM) and different polar protic through apolar aprotic solvents are evident on the calculated $AE_{S-T}$ of the phenyl cation. Electron-donating substituents on the phenyl cation substantially lower the $AE_{S-T}$ to an extent where some functional groups ($-NH_2$, $N(CH_3)_2$, $OCH_3$, and $SCH_3$) can result in triplet ground states depending on their position relative to the cation. In contrast to the phenyl and 1- and 2-naphthyl cations, which are predicted to be ground state singlets, the three parent anthracenyl cations will be ground state triplets.

✉ Sierra Rayne
sierra.rayne@alumni.ubc.ca

[1] Chemologica Research, 1617-11th Avenue NW, Moose Jaw, SK S6H 6M5, Canada

[2] Department of Environmental Engineering Technology, Saskatchewan Polytechnic, 600 Saskatchewan Street West, Moose Jaw, SK S6H 4R4, Canada

**Keywords** Phenyl cations · Substituent effects · Singlet–triplet excitation energies · Ground state multiplicity

## 1 Introduction

The existence and energetics of aryl cations has long been a topic of interest among the organic chemistry community [1–6]. In particular, the nature of the ground state multiplicity for the parent and substituted phenyl cations has attracted considerable attention. The parent system is known to have two low-energy minima which corresponds to the $^1A_1$ and $^3B_1$ states, with the intersection between the lowest energy singlet and triplet hypersurfaces lying close to the triplet geometry and energy [7]. Coupled with non-trivial spin–orbit coupling between these two states near the crossing point [8], the triplet phenyl cation is a short-lived intermediate that rapidly decays [7] to the ground singlet state 102 kJ/mol below the triplet minimum [9]. The phenyl cation has been isolated and characterized in argon [10, 11] and LiCl matrices [12] and in the gas phase [13], and indirectly detected in aqueous solution with a lifetime of <500 ps [14].

The closed-shell singlet state of aryl cations has six π-electrons in the ring and an empty in-plane σ-like orbital on the dicoordinate carbon atom carrying the formal positive charge. In the triplet state, the σ orbital contains an unpaired electron and the ring has only five π-electrons [15]. Where substituents are present, the singlet state is stabilized by σ-donors in the positional order efficacy *ortho* > *meta* > *para* and by π-donors in the order *para* > *ortho* > *meta*, while triplet states are stabilized by π-donors in the order *para* ~ *ortho* > *meta* [16]. The differing spin states display varying chemoselectivity in their

reactivity with nucleophiles [17, 18]. Singlet phenyl cations react rather unspecifically; triplets prefer unsaturated functional groups (π-nucleophiles) over those with lone pairs (n nucleophiles) [19]. The phenyl cation can also be stabilized via hyperconjugation with high-lying strained carbon–carbon bonds [20].

To better understand and predict experimental behavior, a range of theoretical investigations have considered the magnitude and direction of the singlet–triplet energy gap ($E_{S-T}$) for the parent (reviewed in Ref. [9]) and substituted aryl cations. However, the prior work has generally been conducted using Hartree–Fock (HF) and density functional theory (DFT) methods, and these methods are known to significantly underestimate the $E_{S-T}$ of organic compounds. Consequently, the use of higher-level (e.g., composite) theoretical methods and/or more modern density functionals is required in order to achieve both qualitative and quantitative $E_{S-T}$ predictivity (see, Refs. [9, 21–27] and references therein). As a result, in the current study we undertook a broad examination of the parent and substituted and benzannelated aryl cations with the high-level G4(MP2) and G4 methods, approaches which should yield $E_{S-T}$ estimates at or near thermochemical accuracy.

## 2 Computational details

Composite method calculations were conducted at the G4(MP2) [28], G4 [29], and W1BD [30] levels of theory as employed in Gaussian 09 [31]. Additional calculations were performed at various semiempirical, Hartree–Fock, density functional, Moller–Plesset perturbation, and composite method levels of theory with a range of basis sets. Full reference details for these other methods are provided in our previous work [9], with the exception of the MN12L [32], MN12SX [33], M11L [34], SOGGA11X [35], APF and APFD [36], N12SX [33], and HISSbPBE [37] density functionals and the Def2TZV, Def2TZVP, Def2TZVPP, and QZVP basis sets [38, 39] which are cited herein. Dispersion corrections were applied using the D2 [40] and D3 (with Becke–Johnson damping) [41] versions of Grimme's dispersion approaches. All calculations were conducted either in the gas phase (1 atm.) or solution phase (1 M) at 298.15 K. Solution phase calculations employed the SMD [42], IEF-PCM [43, 44], and C-PCM [45, 46] solvation models. Geometries were visualized using Gabedit 2.4.7 [47] and Avogadro 1.1.1 [48]. Geometry optimizations for all compounds were conducted in both the singlet and triplet state and converged absent imaginary frequencies.

## 3 Results and discussion

Our studies began with a comprehensive investigation into the effects of model chemistry on the calculated adiabatic singlet–triplet excitation energy ($AE_{S-T}$) of the parent phenyl cation. In prior work [9], we investigated well-to-well singlet–triplet excitation energies ($WWE_{S-T}$) using single point calculations on the B3LYP/TZVP optimized geometry (i.e., $WWE_{S-T}$ at the x/TZVP//B3LYP/TZVP level of theory, where x is the model chemistry; semiempirical calculations were at the x//B3LYP/TZVP level). The values reported in Table 1 herein are full geometry optimizations and frequency calculations at the x/TZVP level (or at the semiempirical level), thereby constituting $AE_{S-T}$ estimates.

The $AE_{S-T}$ estimates for the phenyl cation range widely over 186 kJ/mol depending on model chemistry, from −41.6 kJ/mol at the HF/TZVP level up to +144.0 kJ/mol at the MP2/TZVP level. Hartree–Fock is known to give lower energies for triplets, which have smaller correlation energies [49]. Almost all DFT methods cluster between 76 and 97 kJ/mol. The G4 $AE_{S-T}$, which has been previously validated [9] against experimental data with no systematic bias nor absolute deviations greater than 6.5 kJ/mol, is thereby taken as the benchmark method for comparison. There are only two density functionals (e.g., B1B95, M11L) within ±~4 kJ/mol from the G4 benchmark, demonstrating the unlikelihood of achieving accurate $AE_{S-T}$ estimates via almost all DFT methods, including the more modern functionals. In addition, semiempirical methods are poor at predicting $AE_{S-T}$ of these types of compounds, negating their potential utility for large organic structures where the low computational cost of semiempirical approaches is very attractive. The less expensive Gaussian-n composite methods [e.g., G4(MP2), G3, G3(MP2B3), G3(MP2), and G3(B3)] offer comparable accuracy to the G4 levels and may offer promise where G4 calculations are prohibitively time-consuming.

The broad $AE_{S-T}$ range among the various methods is not due to large differences in the geometry of the singlet or triplet phenyl cation between computational approaches. The $C_6$–$C_1$–$C_2$ angle for the singlet state phenyl cation averages 147.6° over all methods with a standard deviation (SD) of only 1.2°. The corresponding triplet state $C_6$–$C_1$–$C_2$ angle averages 127.8° with even less method-dependent variation (SD = 0.5°). Basis set effects (Table 2) on the phenyl cation $AE_{S-T}$ are much smaller than model chemistry impacts, but are still non-negligible. Depending on the basis set chosen, $AE_{S-T}$ may vary by upwards of 13 kJ/mol within a specific model chemistry. Dispersion correction impacts are minimal, resulting in—at most—a few tenths of a kJ/mol change in the $AE_{S-T}$ (Table 3). Similarly, there

**Table 1** Gas phase standard state (298.15 K, 1 atm.) $AE_{S-T}$ and singlet/triplet $C_6$–$C_1$–$C_2$ angles of the parent phenyl cation at the x/TZVP level of theory (where 'x' denotes the model chemistry employed; e.g., "MP2/TZVP")

| Model chemistry | $AE_{S-T}$ (kJ/mol) | $C_6$–$C_1$–$C_2$ angle (°) | | Model chemistry | $AE_{S-T}$ (kJ/mol) | $C_6$–$C_1$–$C_2$ angle (°) | |
|---|---|---|---|---|---|---|---|
| | | Singlet | Triplet | | | Singlet | Triplet |
| MP2 | 144.0 | 148.4 | 127.9 | B98 | 84.8 | 147.5 | 127.8 |
| G1 | 113.1 | 148.9 | 127.7 | B3LYP | 83.9 | 147.2 | 127.7 |
| MN12L | 110.9 | 147.4 | 127.1 | mPW3PBE | 83.5 | 147.9 | 127.8 |
| G2 | 110.7 | 148.9 | 127.7 | X3LYP | 82.8 | 147.3 | 127.7 |
| G2(MP2) | 110.7 | 148.9 | 127.7 | M05 | 82.5 | 148.1 | 128.3 |
| MN12SX | 107.2 | 147.8 | 127.5 | B3PW91 | 82.3 | 147.9 | 127.8 |
| CBS-QB3 | 106.8 | 147.5 | 127.7 | wB97XD | 80.9 | 147.8 | 127.6 |
| M11L | 105.4 | 147.6 | 127.2 | APFD | 80.7 | 148.1 | 128.0 |
| G3(MP2B3) | 103.5 | 147.3 | 127.7 | APF | 80.4 | 148.0 | 127.8 |
| G3(MP2) | 103.2 | 148.9 | 127.7 | N12SX | 79.7 | 147.9 | 127.8 |
| G3(B3) | 102.6 | 147.3 | 127.7 | PBE0 | 79.1 | 148.1 | 127.8 |
| G4(MP2) | 102.0 | 148.2 | 128.0 | TPSSh | 78.8 | 147.7 | 127.8 |
| G3 | 101.9 | 148.9 | 127.7 | BHandH | 78.2 | 148.3 | 127.9 |
| G4 | 101.7 | 148.2 | 128.0 | OHSE1PBE | 77.9 | 147.9 | 127.8 |
| B1B95 | 97.3 | 148.4 | 128.1 | CAM-B3LYP | 77.7 | 147.7 | 127.9 |
| CBS-4M | 95.0 | 144.0 | 125.6 | PBEh1PBE | 77.6 | 148.0 | 127.8 |
| VSXC | 94.1 | 147.1 | 128.3 | mPW1LYP | 77.6 | 147.2 | 127.7 |
| B2PLYP | 93.8 | 147.5 | 127.7 | OHSE2PBE | 77.1 | 147.9 | 127.8 |
| B2PLYLPD | 93.7 | 147.5 | 127.7 | wB97 | 76.9 | 148.0 | 128.1 |
| B2PLYLPD3 | 93.6 | 147.3 | 127.6 | mPW1PBE | 76.6 | 148.1 | 127.8 |
| B972 | 90.6 | 147.8 | 127.9 | B1LYP | 76.6 | 147.3 | 127.7 |
| BMK | 90.0 | 148.0 | 127.8 | mPW1PW91 | 76.2 | 148.0 | 127.7 |
| mPW2PLYP | 89.2 | 147.5 | 127.7 | wB97X | 76.1 | 147.9 | 127.7 |
| mPW2PLYPD | 89.1 | 147.6 | 127.7 | LC-wPBE | 68.5 | 148.7 | 128.0 |
| B971 | 88.8 | 147.6 | 127.8 | HISSbPBE | 61.4 | 148.2 | 127.8 |
| M06L | 88.3 | 147.1 | 127.0 | BHandHLYP | 55.7 | 147.5 | 127.6 |
| tHCTHhyb | 86.9 | 147.5 | 127.9 | AM1 | 7.3 | 141.4 | 129.2 |
| M06 | 86.2 | 147.8 | 127.6 | PM3 | −9.6 | 144.5 | 129.1 |
| B3P86 | 86.0 | 147.8 | 127.8 | PDDG | −9.9 | 145.1 | 129.6 |
| SOGGA11X | 85.5 | 148.0 | 128.0 | HF | −41.6 | 147.2 | 126.6 |

Composite and semiempirical method $AE_{S-T}$ are provided for comparison

are collectively only modest (i.e., several kJ/mol or less) effects of different solvation models (SMD, IEF-PCM, and C-PCM) and different polar protic through apolar aprotic solvents on the calculated $AE_{S-T}$ of the phenyl cation (Table 4).

G4(MP2) and G4 calculations were used to probe the effects when a range of electron-withdrawing and releasing substituents were placed in the *ortho*-, *meta*-, and *para*-positions relative to the phenyl cation (Table 5). For the hydroxy, thiol, methoxy, and thiomethoxy substituents, both *anti*- and *syn*- conformations are possible (Fig. 1). In all cases, the *ortho–anti* conformation $AE_{S-T}$ is higher (generally by several kJ/mol) than the corresponding *ortho–syn* conformation $AE_{S-T}$, but these effects are minor relative to the difference between substituents and near the error of the computational methods. Earlier work [16] using low-level STO-3G calculations reported a stable higher energy orthogonal geometry for the amino substituent in the *ortho*-, *meta*-, and *para*-positions. We were unable to reproduce these findings at the G4(MP2) and G4 levels. All substituents assumed a planar configuration with respect to the phenyl moiety regardless of position on the ring or starting conformation.

Previous investigations [15, 16, 50, 51] at lower levels of theory predicted that *meta*-substituted amino- and thiomethoxy-phenyl cations—as well as the *para*-substituted methoxy-, thio-, and hydroxy-phenyl cations—would all be triplet ground states, whereas the G4(MP2) and G4 calculations suggest these will be singlet ground states. As Bondarchuk and Minaev [52] (B3LYP/6-31G(d,p)) and

**Table 2** Gas phase standard state (298.15 K, 1 atm.) $AE_{S-T}$ of the parent phenyl cation using various Pople, Dunning, and Ahlrichs basis sets with the HF, PBE0, wB97XD, MN12SX, and MP2 model chemistries

| Basis set | Model chemistry | | | | |
|---|---|---|---|---|---|
| | HF | PBE0 | wB97XD | MN12SX | MP2 |
| 6-311++G(d,p) | −41.3 | 79.5 | 81.6 | 106.9 | 151.9 |
| 6-311++G(3df,2pd) | −36.6 | 83.9 | 85.7 | 108.7 | 148.6 |
| cc-pVDZ | −42.7 | 77.1 | 78.8 | 106.9 | 151.6 |
| cc-pVTZ | −36.0 | 84.6 | 86.4 | 111.2 | 148.2 |
| cc-pVQZ | −35.7 | 84.7 | 86.7 | 109.2 | c/e[a] |
| AUG-cc-pVTZ | −36.0 | 84.5 | 86.1 | 110.3 | 150.2 |
| TZV | −44.0 | 72.2 | 74.9 | 100.9 | n/c[b] |
| TZVP | −41.6 | 79.1 | 80.9 | 107.2 | 144.0 |
| Def2TZV | −44.0 | 72.2 | 74.9 | 100.9 | n/c |
| Def2TZVP | −35.9 | 84.1 | 86.0 | 110.9 | 148.8 |
| Def2TZVPP | −36.0 | 84.2 | 86.1 | 111.1 | 148.9 |
| QZVP | −35.7 | 84.6 | 86.5 | 108.7 | c/e |

Values are in kJ/mol

[a] Not completed due to computational expense

[b] The triplet state phenyl cation failed to converge absent any imaginary frequencies despite repeated attempts, including using the converged TZVP geometry as input

**Table 3** Gas phase standard state (298.15 K, 1 atm.) $AE_{S-T}$ of the parent phenyl cation at the x/TZVP level of theory with and without dispersion corrections for representative model chemistries

| Model chemistry | $AE_{S-T}$ |
|---|---|
| LC-wPBE | 68.5 |
| LC-wPBE-D3 | 68.2 |
| CAM-B3LYP | 77.7 |
| CAM-B3LYP-D3 | 77.5 |
| PBE0 | 79.1 |
| PBE0-D3 | 78.8 |
| B3PW91 | 82.3 |
| B3PW91-D3 | 81.8 |
| B3LYP | 83.9 |
| B3LYP-D3 | 83.6 |
| mPW2PLYP | 89.2 |
| mPW2PLYP-D | 89.1 |
| BMK | 90.0 |
| BMK-D3 | 89.7 |
| B2PLYP | 93.8 |
| B2PLYLP-D | 93.7 |
| B2PLYLP-D3 | 93.6 |

Values are in kJ/mol

Lazzaroni et al. [50] (UB3LYP/6-31G(d)) have previously shown, the singlet *o*-nitrophenyl cation cannot likely exist in the gas phase since calculations lead to a rearranged structure. At the G4(MP2) and G4 levels, we are able to reproduce these findings, obtaining a ring-opened species via intramolecular oxygen transfer to the carbocation from starting geometries where the nitro group was in-plane and orthogonal to the aryl moiety.

Electron-donating substituents on the phenyl cation lower the $AE_{S-T}$, following a general pattern that correlates significantly ($p < 0.05$)—but having less than desirable predictivity—with the corresponding Hammett [53] $\sigma_m$ and $\sigma_p$ (Fig. 2a) and $\sigma_p^+$ (Fig. 2b) substituent constants. Other researchers have observed this via theoretical studies [15, 16]. Cox et al. [54] experimentally observed a triplet ground state for the *p*-dimethylaminophenyl cation. At the G4 level, we calculate $AE_{S-T}$ of −30.4, 18.0, and −36.6 kJ/mol for the *ortho*-, *meta*-, and *para*-substituted dimethylaminophenyl cation derivatives, in support of the experimental claims for a *para*-substituted triplet ground state.

In a series of experimental studies on substituted phenyl cations, Ambroz et al. [55–57] reported that the 3-methoxy, 4-methoxy, 2,4-dimethoxy, 3,5-dimethoxy, 3,4,5-trimethoxy, 2,4,6-trimethoxy, 3,4-dichloro, 2,4,5-trichloro, and 2,4,6-tribromo substituted phenyl cations were likely singlet ground states, whereas the 2,4,5-trimethoxy and 3,5-dichloro-5-amino substituted phenyl cations were probably ground state triplets. At the G4(MP2) level, our calculations support the assignment of the 3,5-dichloro-5-amino ($AE_{S-T}$ = −32.4 kJ/mol) and 2,4,5-trimethoxy ($AE_{S-T}$ = −34.3 kJ/mol) derivatives as ground state triplets, as well as the 3,5-dimethoxy ($AE_{S-T}$ = 43.6 kJ/mol), 2,4,6-trimethoxy ($AE_{S-T}$ = 6.4 kJ/mol), 3,4-dichloro ($AE_{S-T}$ = 38.4 kJ/mol), and 2,4,6-tribromo ($AE_{S-T}$ = 9.1 kJ/mol) derivatives as ground state singlets. On the other hand, G4(MP2) calculations suggest the 2,4-dimethoxy ($AE_{S-T}$ = −33.8 kJ/mol), 3,4,5-trimethoxy ($AE_{S-T}$ = −27.1 kJ/mol), and 2,4,5-trichloro ($AE_{S-T}$ = −4.5 kJ/mol) derivatives will be ground state triplets rather than singlets, although the computational error for the 2,4,5-trichlorophenyl cation $AE_{S-T}$ leaves room for potential singlet–triplet isoenergicity.

To investigate the potential generalizability of these structure–property substituent trends, the $AE_{S-T}$ of various silylenes was calculated via the G4 and W1BD methods (Table 6). At these levels of theory, we obtain $AE_{S-T}$ which are in reasonable agreement with previously published [58] CCSD(T)/6-311++G(d,p)//QCISD/6-31G(d) [G4 mean signed deviation (MSD) = 7.5, mean absolute deviation (MAD) = 7.5, and root mean squared deviation (RMSD) = 8.4; W1BD MSD = 5.0, MAD = 5.0, and RMSD = 5.4; all values in kJ/mol] and B3LYP/AUG-cc-pVTZ//B3LYP/6-31+G(d) (G4 MSD = 15.5, MAD = 15.5, and RMSD = 15.9; W1BD MSD = 13.4, MAD = 1.4, and RMSD = 13.8; all values in kJ/mol) $E_{S-T}$

**Table 4** Standard state $AE_{S-T}$ of the parent phenyl cation at the G4(MP2) and G4 levels of theory in various solvents (298.15 K, 1 M) using the SMD, IEF-PCM, and C-PCM solvation models

| Gas | G4(MP2) 102.0 | | | G4 101.7 | | |
|---|---|---|---|---|---|---|
| | SMD | IEF-PCM | C-PCM | SMD | IEF-PCM | C-PCM |
| Water | 107.0 | 103.5 | 103.5 | 106.4 | 106.8 | 102.9 |
| Acetonitrile | 106.5 | 103.5 | 103.4 | 106.0 | 102.9 | 102.9 |
| DMSO | 106.8 | 103.5 | 103.5 | 106.2 | 102.9 | 102.9 |
| Dichloromethane | 105.8 | 103.4 | 103.3 | 105.2 | 102.9 | 102.8 |
| Methanol | 106.7 | 103.5 | 103.4 | 106.1 | 102.9 | 102.9 |
| Benzene | 104.1 | 103.0 | 102.8 | 103.6 | 102.5 | 102.3 |
| Cyclohexane | 103.8 | 102.9 | 102.7 | 103.4 | 102.5 | 102.3 |
| Argon | 103.0 | 102.6 | 102.4 | 102.6 | 102.2 | 102.0 |

Values are in kJ/mol

**Table 5** Gas phase standard state (298.15 K, 1 atm.) $AE_{S-T}$ of substituted phenyl cations at the G4(MP2) and G4 levels of theory

| Substituent | G4(MP2) | | | G4 | | |
|---|---|---|---|---|---|---|
| | *Ortho* | *Meta* | *Para* | *Ortho* | *Meta* | *Para* |
| –H | 102.0 | 102.0 | 102.0 | 101.7 | 101.7 | 101.7 |
| –F | 29.7 | 70.6 | 56.4 | 29.7 | 71.4 | 57.0 |
| –Cl | 48.0 | 66.2 | 53.7 | 47.4 | 66.5 | 53.0 |
| –Br | 50.6 | 63.7 | 49.9 | 50.1 | 63.9 | 49.2 |
| $–NH_2$ | −26.9 | 19.6 | −23.2 | −29.4 | 17.8 | −25.4 |
| $–N(CH_3)_2$ | −28.2 | 18.9 | −35.2 | −30.4 | 18.0 | −36.6 |
| $–NO_2$ | n/a[b] | 103.5 | 93.2 | n/a[b] | 104.1 | 95.0 |
| –OH[a] | 12.1/5.7 | 44.1/39.4 | 19.2 | 11.1/4.3 | 44.1/39.4 | 18.2 |
| –SH[a] | 15.1/12.9 | 26.3/23.7 | 4.4 | 14.5/12.1 | 26.5/24.2 | 3.5 |
| $–OCH_3$[a] | 0.4/−2.3 | 36.1/33.1 | 4.7 | −0.1/−3.3 | 36.5/33.7 | 4.3 |
| $–SCH_3$[a] | −4.3/−10.6 | 12.9/16.5 | −17.2 | −4.2/−10.8 | 13.4/16.6 | −17.7 |
| $–CH_3$ | 89.9 | 85.5 | 69.4 | 89.6 | 85.8 | 71.0 |
| $–CF_3$ | 81.6 | 92.1 | 95.9 | 84.6 | 95.1 | 99.1 |
| –CN | 78.8 | 95.0 | 87.2 | 78.8 | 94.6 | 87.3 |
| –C≡CH | 53.6 | 61.4 | 47.5 | 52.4 | 61.4 | 46.4 |
| $–C_6H_5$ | 24.6 | 36.8 | 17.9 | c/e[c] | c/e | c/e |

Values are in kJ/mol

[a] For the *ortho*- and *meta*-positions, values are presented as *anti*/*syn* conformers (Fig. 1)

[b] Singlet state cation rearranged to ring-opened species via intramolecular oxygen transfer to the carbocation from starting geometries where the nitro group was in-plane and orthogonal to the aryl moiety

[c] Not completed due to computational expense

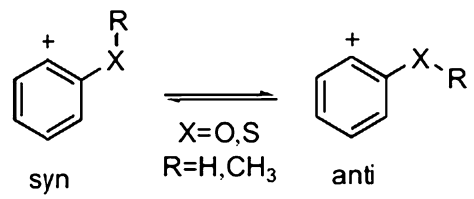


**Fig. 1** Structures of the *syn*- and *anti*-conformations for the hydroxy (X=O, R=H), thiol (X=S, R=H), methoxy (X=O, R=$CH_3$), and thiomethoxy (X=S, R=$CH_3$) substituted phenyl cations

results. However, both the CCSD(T)/6-311++G(d,p)//QCISD/6-31G(d) and B3LYP/AUG-cc-pVTZ//B3LYP/6-31+G(d) methods offer systematically lower $E_{S-T}$ than the G4 and W1BD values by between about 4–20 kJ/mol (averaging about 4–8 and 13–17 kJ/mol negative deviations, respectively) depending on the compound/method combination.

The $H_2C$=Si, $H_2Si$=Si, HN=Si, $(H_3C)HSi$=Si, and $(H_3C)_2Si$=Si silylenes are consistently predicted to clearly be ground state singlets using the G4, W1BD (with the

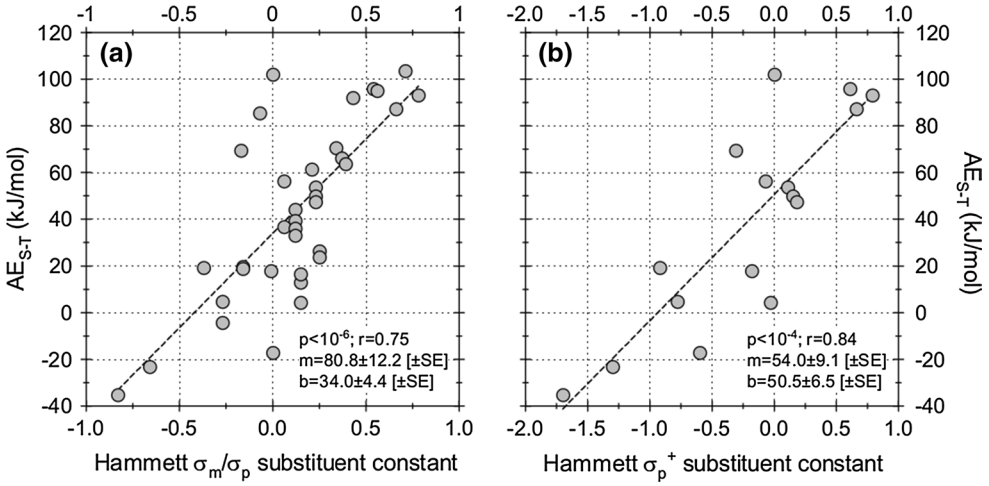


**Fig. 2** Correlations between the gas phase standard state (298.15 K, 1 atm.) $AE_{S-T}$ of substituted phenyl cations from Table 5 calculated at the G4(MP2) level and the corresponding Hammett (**a**) $\sigma_m$ and $\sigma_p$ and (**b**) $\sigma_p^+$ substituent constants

**Table 6** Gas phase standard state (298.15 K, 1 atm.) $AE_{S-T}$ of various silylenes at the G4 and W1BD levels of theory

| Compound | G4 | W1BD |
|---|---|---|
| $H_2C{=}Si$ | 169.5 | 165.3 |
| $H_2Si{=}Si$ | 48.1 | 42.3 |
| $HN{=}Si$ | 342.3 | 341.8 |
| $(H_3C)HSi{=}Si$ | 36.0 | 31.8 |
| $(H_2N)HSi{=}Si$ | −10.0 | −13.0 |
| $(HO)HSi{=}Si$ | 2.5 | −1.3 |
| $FHSi{=}Si$ | 7.9 | 3.8 |
| $(H_3C)_2Si{=}Si$ | 25.9 | c/e[a] |
| $(H_2N)_2Si{=}Si$ | −37.7 | c/e |
| $(HO)_2Si{=}Si$ | −36.4 | −38.1 |
| $F_2Si{=}Si$ | −16.3 | −18.8 |

Values are in kJ/mol

[a] Not completed due to computational expense

**Table 7** Gas phase standard state (298.15 K, 1 atm.) $AE_{S-T}$ of the phenyl, naphthyl, and anthracenyl cations at the G4(MP2) and G4 levels of theory

| Cation | G4(MP2) | G4 |
|---|---|---|
| Phenyl | 102.0 | 101.7 |
| 1-Naphthyl | 17.7 | 19.3 |
| 2-Naphthyl | 20.7 | 21.0 |
| 1-Anthracenyl | −29.4 | c/e[a] |
| 2-Anthracenyl | −24.8 | c/e |
| 9-Anthracenyl | −40.4 | c/e |

Values are in kJ/mol

[a] Not completed due to computational expense

exception of $(H_3C)_2Si{=}Si$, for which the calculation cost was too expensive), CCSD(T)/6-311++G(d,p)//QCISD/6-31G(d), and B3LYP/AUG-cc-pVTZ//B3LYP/6-31+G(d) methods, analogous to the prediction of clear triplet ground states for $(H_2N)HSi{=}Si$, $(H_2N)_2Si{=}Si$, $(HO)_2Si{=}Si$, and $F_2Si{=}Si$ using all four levels of theory (with the exception of $(H_2N)_2Si{=}Si$, for which W1BD calculations were too computationally expensive). However, there is disagreement as to the ground state multiplicity for $(HO)HSi{=}Si$ and $FHSi{=}Si$ using the different theoretical methods. The CCSD(T)/6-311++G(d,p)//QCISD/6-31G(d) and B3LYP/AUG-cc-pVTZ//B3LYP/6-31+G(d) methods predict $(HO)HSi{=}Si$ will be a ground state triplet, whereas the G4 and W1BD methods predict either a slightly energetically favored ground state singlet (G4) or an energetic degeneracy between the two multiplicities (W1BD). For $FHSi{=}Si$, both the G4 and W1BD methods predict a clear ground state singlet, whereas the CCSD(T)/6-311++G(d,p)//QCISD/6-31G(d) method predicts effective energetic degeneracy, and the B3LYP/AUG-cc-pVTZ//B3LYP/6-31+G(d) method predicts a clear ground state triplet. Overall, the phenyl cations and silylenes display analogous structure–property substituent patterns, with an $AE_{S-T}$ ordering trend of parent > methyl > fluoro > hydroxy > amino and multiple substitutions further lowering the $AE_{S-T}$ below the monosubstituted compound.

In contrast to the unsubstituted phenyl and naphthyl cations, which will clearly be ground state singlets [9], the 1-, 2-, and 9-anthracenyl cations will be ground state triplets, having $AE_{S-T}$ of −29.4, −24.8, and −40.4 kJ/mol, respectively (Table 7). Laali et al. [51] reported a $E_{S-T}$ gap of −56 kJ/mol at the B3LYP/6-311+G(d)//B3LYP/6-311+G(d) level for the 9-anthracenyl cation. Our value is about 16 kJ/mol higher, but in qualitative agreement.

The nature and magnitude of the singlet–triplet transition for phenyl cations has important practical implications. For example, correlations between $E_{S-T}$ gaps for unsaturated compounds and yields of the corresponding Meerwein reaction products have been reported [59], thereby offering mechanistic insights that may be extended to other systems.

In addition, the current findings support prior theoretical work explaining why aryl cations have differing ground state multiplicities depending on the type and location of substituents. The singlet ground state and two ($^3B_1$, $^3A_2$) low-lying triplet excited states are known to have different geometric and electronic structures [49]. For the singlet, the positive charge resides in the σ system; however, for the triplets the cation is delocalized throughout the π system. With π-acceptor substituents (including the parent phenyl cation), singlet ground states occur. As substituents become increasingly π-donating, the triplet ground state becomes increasingly favorable. In general, it can be summarized that singlet phenyl cations are best stabilized by σ-donating substituents in the positional order *ortho* > *meta* > *para*, with π-donors being effective in the expected resonance-based ordering pattern *para* > *ortho* > *meta*. On the other hand, π-donors also stabilize the triplet state in the order *para* ~ *ortho* > *meta*, and for strong π-donors such as the amino moiety, the relative stabilization of the triplet far exceeds that of the singlet, resulting in a ground state triplet [16]. An examination of the aryl cation $E_{S-T}$ substituent trends presented herein at the G4 level shows excellent agreement with this theoretical framework.

**Acknowledgments** This work was made possible by the facilities of the Western Canada Research Grid (WestGrid: project 100185), the Shared Hierarchical Academic Research Computing Network (SHARCNET: project sn4612), and Compute/Calcul Canada.

## References

1. Lewis ES (1958) Reactivity of the phenyl cation in solution. J Am Chem Soc 80:1371–1373
2. Taft RW (1961) Evidence for phenyl cation with an odd number of π-electrons from the aqueous thermal decomposition of the diazonium ion. J Am Chem Soc 83:3350–3351
3. Swain CG, Sheats JE, Harbison KG (1975) Evidence for phenyl cation as an intermediate in reactions of benzenediazonium salts in solution. J Am Chem Soc 97:783–790. doi:10.1021/ja00837a016
4. Guizzardi B, Mella M, Fagnoni M, Albini A (2003) Photochemical reaction of *N*, *N*-dimethyl-4-chloroaniline with dienes: new synthetic paths via a phenyl cation. Chem Eur J 9:1549–1555
5. Bergstrom RG, Landells RGM, Wahl GH, Zollinger H (1976) Dediazoniation of arenediazonium ions in homogeneous solution. 7. On the intermediacy of the phenyl cation. J Am Chem Soc 98:3301–3305
6. Ambroz HB, Kemp TJ (1979) Aryl cations—new light on old intermediates. Chem Soc Rev 8:353–365. doi:10.1039/CS9790800353
7. Harvey JN, Aschi M, Schwarz H, Koch W (1998) The singlet and triplet states of phenyl cation. A hybrid approach for locating minimum energy crossing points between non-interacting potential energy surfaces. Theor Chem Acc 99:95–99. doi:10.1007/s002140050309
8. Hrusak J, Schröder D, Iwata S (1997) The ground state ($^1A_1$) and the lowest triplet state ($^3B_1$) of the phenyl cation $C_6H_5^+$ revisted. J Chem Phys 106:7541–7549. doi:10.1063/1.473757
9. Rayne S, Forest K (2012) Singlet–triplet excitation energies of naphthyl cations: high level composite method calculations suggest a singlet ground state. Comput Theor Chem 983:69–75. doi:10.1016/j.comptc.2012.01.005
10. Winkler M, Sander W (2000) Isolation of the phenyl cation in a solid argon matrix. Angew Chem Int Ed 39:2014–2016. doi:10.1002/1521-3773(20000602)39:11<2014:AID-ANIE2014>3.0.CO;2-E
11. Winkler M, Sander W (2006) Generation and reactivity of the phenyl cation in cryogenic argon matrices: monitoring the reactions with nitrogen and carbon monoxide directly by IR spectroscopy. J Org Chem 71:6357–6367. doi:10.1021/jo0603678
12. Ambroz HB, Przybytniak GK, Stradowski CZ, Wolszczak M (1990) Optical spectroscopy of the aryl cation, the intermediate in the decomposition of arenediazonium salts. J Photochem Photobiol Chem 52:369–374
13. Patzer A, Chakraborty S, Solcà N, Dopfer O (2010) IR spectrum and structure of the phenyl cation. Angew Chem Int Ed 49:10145–10148. doi:10.1002/anie.201006357
14. Scaiano JC, Kim-Thuan N (1983) Diazonium salts in photochemistry III. Attempts to characterize aryl cations. J Photochem 23:269–276
15. Aschi M, Harvey JN (1999) Spin isomerisation of *para*-substituted phenyl cations. J Chem Soc Perkin Trans 2:1059–1062
16. Dill JD, Schleyer PVR, Pople JA (1977) Molecular orbital theory of the electronic structure of molecules. 31. Substituent stabilization of the phenyl cation. J Am Chem Soc 99:1–8
17. Milanesi S, Fagnoni M, Albini A et al (2003) Cationic arylation through photo(sensitised) decomposition of diazonium salts. Chemoselectivity of triplet phenyl cations. Chem Commun 216–217
18. Protti S, Dichiarante V, Dondi D et al (2012) Singlet/triplet phenyl cations and benzyne from the photodehalogenation of some silylated and stannylated phenyl halides. Chem Sci 3:1330–1337. doi:10.1039/c2sc20060k
19. Slegt M, Overkleeft HS, Lodder G (2007) Fingerprints of singlet and triplet phenyl cations. Eur J Org Chem 32:5364–5375. doi:10.1002/ejoc.200700339
20. Apeloig Y, Arad D (1985) Stabilization of the phenyl cation by hyperconjugation. J Am Chem Soc 107:5285–5286. doi:10.1021/ja00304a049
21. Nicolaides A, Smith DM, Jensen F, Radom L (1997) Phenyl radical, cation, and anion. The triplet–singlet gap and higher excited states of the phenyl cation. J Am Chem Soc 119:8083–8088. doi:10.1021/ja970808s
22. Gronert S, Keeffe JR, More O'Ferrall RA (2011) Stabilities of carbenes: independent measures for singlets and triplets. J Am Chem Soc 133:3381–3389. doi:10.1021/ja1071493
23. Winter AH, Falvey DE (2010) Vinyl cations substituted with beta π-donor have triplet ground states. J Am Chem Soc 132:215–222
24. Zhou X, Hrovat DA, Gleiter R, Borden WT (2009) Reinvestigation of the ordering of the low-lying electronic states of cyclobutanetetraone with CASPT2, CCSD(T), G3B3, ccCA, and CBS-QB3 calculations. Mol Phys 107:863–870. doi:10.1080/00268970802672650
25. Woodcock HL, Moran D, Brooks BR et al (2007) Carbene stabilization by aryl substituents. Is bigger better? J Am Chem Soc 129:3763–3770. doi:10.1021/ja068899t
26. Rayne S, Forest K (2011) A comparison of density functional theory (DFT) methods for estimating the singlet–triplet ($S_0$–$T_1$) excitation energies of benzene and polyacenes. Comput Theor Chem 976:105–112. doi:10.1016/j.comptc.2011.08.010
27. Rayne S, Forest K (2011) Singlet–triplet ($S_0 \rightarrow T_1$) excitation energies of the [4 × n] rectangular graphene nanoribbon series (n = 2–6): a comparative theoretical study. Comput Theor Chem 977:163–167. doi:10.1016/j.comptc.2011.09.021

28. Curtiss LA, Redfern PC, Raghavachari K (2007) Gaussian-4 theory using reduced order perturbation theory. J Chem Phys 127:124105. doi:10.1063/1.2770701
29. Curtiss LA, Redfern PC, Raghavachari K (2007) Gaussian-4 theory. J Chem Phys 126:084108. doi:10.1063/1.2436888
30. Barnes EC, Petersson GA, Montgomery JA et al (2009) Unrestricted coupled cluster and Brueckner doubles variations of W1 theory. J Chem Theory Comput 5:2687–2693. doi:10.1021/ct900260g
31. Frisch MJ, Trucks GW, Schlegel HB et al (2009) Gaussian 09, revision D01. Gaussian Inc, Wallingford
32. Peverati R, Truhlar DG (2012) An improved and broadly accurate local approximation to the exchange–correlation density functional: the MN12-L functional for electronic structure calculations in chemistry and physics. Phys Chem Chem Phys 14:13171–13174. doi:10.1039/c2cp42025b
33. Peverati R, Truhlar DG (2012) Screened-exchange density functionals with broad accuracy for chemistry and solid-state physics. Phys Chem Chem Phys 14:16187–16191. doi:10.1039/C2CP42576A
34. Peverati R, Truhlar DG (2012) M11-L: a local density functional that provides improved accuracy for electronic structure calculations in chemistry and physics. J Phys Chem Lett 3:117–124. doi:10.1021/jz201525m
35. Peverati R, Truhlar DG (2011) A global hybrid generalized gradient approximation to the exchange–correlation functional that satisfies the second-order density-gradient constraint and has broad applicability in chemistry. J Chem Phys 135:191102. doi:10.1063/1.3663871
36. Austin A, Petersson GA, Frisch MJ et al (2012) A density functional with spherical atom dispersion terms. J Chem Theory Comput 8:4989–5007. doi:10.1021/ct300778e
37. Henderson TM, Izmaylov AF, Scuseria GE, Savin A (2008) Assessment of a middle-range hybrid functional. J Chem Theory Comput 4:1254–1262. doi:10.1021/ct800149y
38. Weigend F, Ahlrichs R (2005) Balanced basis sets of split valence, triple zeta valence and quadruple zeta valence quality for H to Rn: design and assessment of accuracy. Phys Chem Chem Phys 7:3297–3305. doi:10.1039/b508541a
39. Weigend F (2006) Accurate Coulomb-fitting basis sets for H to Rn. Phys Chem Chem Phys 8:1057–1065. doi:10.1039/b515623h
40. Grimme S (2006) Semiempirical GGA-type density functional constructed with a long-range dispersion correction. J Comput Chem 27:1787–1799
41. Grimme S, Ehrlich S, Goerigk L (2011) Effect of the damping function in dispersion corrected density functional theory. J Comput Chem 32:1456–1465
42. Marenich AV, Cramer CJ, Truhlar DG (2009) Universal solvation model based on solute electron density and on a continuum model of the solvent defined by the bulk dielectric constant and atomic surface tensions. J Phys Chem B 113:6378–6396. doi:10.1021/jp810292n
43. Tomasi J, Mennucci B, Cammi R (2005) Quantum mechanical continuum solvation models. Chem Rev 105:2999–3093. doi:10.1021/cr9904009
44. Scalmani G, Frisch MJ (2010) Continuous surface charge polarizable continuum models of solvation. I. General formalism. J Chem Phys 132:114110. doi:10.1063/1.3359469
45. Cossi M, Rega N, Scalmani G, Barone V (2003) Energies, structures, and electronic properties of molecules in solution with the C-PCM solvation model. J Comput Chem 24:669–681. doi:10.1002/jcc.10189
46. Barone V, Cossi M (1998) Quantum calculation of molecular energies and energy gradients in solution by a conductor solvent model. J Phys Chem A 102:1995–2001. doi:10.1021/jp9716997
47. Allouche A-R (2011) Gabedit: a graphical user interface for computational chemistry softwares. J Comput Chem 32:174–182
48. Hanwell MD, Curtis DE, Lonie DC et al (2012) Avogadro: an advanced semantic chemical editor, visualization, and analysis platform. J Cheminform 4:17. doi:10.1186/1758-2946-4-17
49. Dill JD, Schleyer PR, Binkley JS et al (1976) Molecular orbital theory of the electronic structure of molecules. 30. Structure and energy of the phenyl cation. J Am Chem Soc 98:5428–5431. doi:10.1021/ja00434a002
50. Lazzaroni S, Dondi D, Fagnoni M, Albini A (2008) Geometry and energy of substituted phenyl cations. J Org Chem 73:206–211. doi:10.1021/jo7020218
51. Laali KK, Rasul G, Prakash GKS, Olah GA (2002) DFT study of substituted and benzannelated aryl cations: substituent dependency of singlet/triplet ratio. J Org Chem 67:2913–2918. doi:10.1021/jo020084p
52. Bondarchuk SV, Minaev BF (2011) Density functional study of *ortho*-substituted phenyl cations in polar medium and in the gas phase. Chem Phys 389:68–74. doi:10.1016/j.chemphys.2011.08.005
53. Hansch C, Leo A, Taft RW (1991) A survey of Hammett substituent constants and resonance and field parameters. Chem Rev 91:165–195. doi:10.1002/chin.199139332
54. Cox A, Kemp TJ, Payne DR et al (1978) Electron spin resonance characterization of ground state triplet aryl cations substituted at the 4 position by dialkylamino groups. J Am Chem Soc 100:4779–4783
55. Ambroz HB, Kemp TJ, Przybytniak GK (1997) Unusual features in the triplet state EPR spectrum of 3,5-dichloro-4-aminophenyl cation. J Photochem Photobiol Chem 108:149–153
56. Ambroz HB, Kemp TJ (1979) Triplet state E.S.R. studies of aryl cations. Part 2. Substituent factors influencing net stabilisation of the triplet level. J Chem Soc Perkin Trans 2:1420–1424
57. Ambroz HB, Kemp TJ, Przybytniak GK (1992) Optical spectroscopy of the aryl cation. 3. Substituent effects on the production and electronic spectra of intermediates in the photodecomposition of $ArN_2^+$; optical characterization of the reaction $Ar^+ + N_2 \rightarrow ArN_2^+$. J Photochem Photobiol Chem 68:85–95
58. Momeni MR, Shakib FA (2011) Theoretical description of triplet silylenes evolved from $H_2Si{=}Si$. Organometallics 30:5027–5032. doi:10.1021/om200586d
59. Bondarchuk SV, Minaev BF (2010) About possibility of the triplet mechanism of the Meerwein reaction. J Mol Struct Theochem 952:1–7. doi:10.1016/j.theochem.2010.04.025